



**HAL**  
open science

## Formation and highly directional output of long-lived resonances in photonic comblike structures

Leonard Dobrzyński, Housni Al-Wahsh, Abdellatif Akjouj, Eman Abdel-Ghaffar

► **To cite this version:**

Leonard Dobrzyński, Housni Al-Wahsh, Abdellatif Akjouj, Eman Abdel-Ghaffar. Formation and highly directional output of long-lived resonances in photonic comblike structures. *Physical Review B*, 2023, 108 (11), pp.115426. 10.1103/PhysRevB.108.115426 . hal-04214111

**HAL Id: hal-04214111**

**<https://hal.science/hal-04214111>**

Submitted on 21 Sep 2023

**HAL** is a multi-disciplinary open access archive for the deposit and dissemination of scientific research documents, whether they are published or not. The documents may come from teaching and research institutions in France or abroad, or from public or private research centers.

L'archive ouverte pluridisciplinaire **HAL**, est destinée au dépôt et à la diffusion de documents scientifiques de niveau recherche, publiés ou non, émanant des établissements d'enseignement et de recherche français ou étrangers, des laboratoires publics ou privés.


## Formation and highly directional output of long-lived resonances in photonic comblike structures

Leonard Dobrzyński 


*Institut d'Electronique, de Microélectronique et de Nanotechnologie (IEMN), UMR CNRS 8520,  
Département de Physique, Université de Lille, 59655 Villeneuve d'Ascq Cédex, France*

Housni Al-Wahsh 

*Engineering Mathematics and Physics Department, Faculty of Engineering,  
Benha University, Shoubra 11629 Cairo, Egypt  
and Institut d'Electronique, de Microélectronique et de Nanotechnologie (IEMN), UMR CNRS 8520,  
Département de Physique, Université de Lille, 59655 Villeneuve d'Ascq Cédex, France*

Abdellatif Akjouj 

*Institut d'Electronique, de Microélectronique et de Nanotechnologie (IEMN), UMR CNRS 8520,  
Département de Physique, Université de Lille, 59655 Villeneuve d'Ascq Cédex, France*

Eman A. Abdel-Ghaffar 

*Electrical Engineering Department, Faculty of Engineering, Benha University, Shoubra 11629 Cairo, Egypt*



(Received 20 March 2023; revised 1 September 2023; accepted 5 September 2023; published 18 September 2023)

Bound states in the continuum (BICs) and long-lived resonances have become a unique way to produce the extreme localization of light waves. In this paper, we present a theoretical demonstration of BICs and long-lived resonances in photonic comblike structures with two semi-infinite leads, together with their existence conditions. The comb structure is composed of connected guides of length  $L$ . The BICs correspond to localized resonances of infinite lifetime inside the comb, without any leakage into the surrounding leads. When BICs exist within state continua, they induce long-lived resonances for specific values of some modified lengths of the guides constituting the comb structure. This enables to regulate these resonances by means of these lengths. The obtained results take due account of the state number conservation between the final system and the reference one constituted by the independent comb and semi-infinite leads. This conservation rule enables to find all the states of the final system and among them the bound in continuum ones. In addition, we present a comb structure with highly directional outputs through two different lines. In each output line two different long-lived resonances enable to transmit two different signals. This system enables to demultiplex two different signals through each of two output lines. The analytical results are obtained by means of the Green's function technique. The structures and the long-lived resonances presented in this paper may have potential applications due to their high sensitivities to weak perturbations, in particular in filtering, sensing, and communication technology improvements.

DOI: [10.1103/PhysRevB.108.115426](https://doi.org/10.1103/PhysRevB.108.115426)

### I. INTRODUCTION

Classical and quantum finite systems have discrete states. Without dissipation, the states have an infinite lifetime. A discrete state in interaction with a state continuum induces at least one resonance. It may also remain a discrete bound in continuum (BIC) state [1]. When a resonance passing band is confined by one or two zeros it is a long-lived resonance [2–5].

Recently bound states in the continuum, also known as trapped modes, have brought significant attention due to their important design principle to create systems with long-lived resonances in order to enhance photon-matter interaction [6]. A BIC state can be considered as resonance with zero linewidth in a lossless system. It resides within the state continua but remain perfectly confined in some parts of the system (subsystem). BICs were first predicted

by Neumann and Wigner in 1929 [1]. Since then, BICs were found in various fields of physics such as photonics [7,8], acoustics [9–11], magnonics [12], mesoscopics [13,14], and plasmonics [15–17]. Interest in BICs also results from their potential use in many applications such as lasers [18], filters [19,20], and sensors [21,22]. BICs can be classified into several mechanisms based on their physical origin [6], e.g., symmetry-protected BICs, Fabry-Perot (FP) BICs, and Friedrich-Wintgen BICs, which have been subsequently investigated theoretically and experimentally in different physical systems [23–26]. By slightly changing the geometrical parameters of the system, the BIC states induce a long-lived resonances.

The comb structure is composed of connected guides attached to semi-infinite leads, see Fig. 1. A similar comb structure appeared recently [27]. This preliminary structure

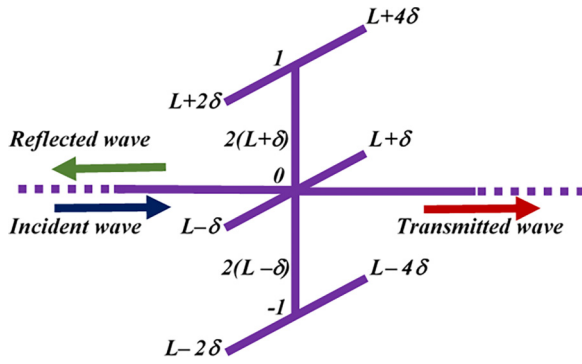


FIG. 1. The two arm three port comb structure. The length of each guide is indicated on the figure. The points  $-1$ ,  $0$ , and  $1$  are the points of connections of the guides with each other and with the semi-infinite leads. This is why we call them *interface points*. The interface space of this structure is written shortly as  $M = \{-1, 0, 1\}$ .

is improved in this paper, with new symmetry breaks. The present structure is shown here below to reveal one more long-lived resonance as the former one. The analysis of all physical properties is also more complete here. This system is shown to have bound in subsystem discrete states.

No state can interact with another state through one of its eigenfunction zero [28,29]. With the leads, some of these states become BICs, or semi-infinite bound states in the continuum (SIBIC) states. A SIBIC state is a state of a semi-infinite subspace bounded within the space continuum of another subspace [27,30]. All BIC states may induce, after some symmetry break, long-lived resonances and SIBIC states. These results are obtained by means of the interface response theory [31], which enables also to deduce the state phase shifts, the variations of the density of states, the transmission, the transmission phase, and the transmission phase time. Any final system can be build out of disconnected pieces called reference system. The number of states is conserved in the building process. This is the state number conservation rule [27,28]. The results presented in this paper take due account of the state number conservation between the final system and the reference one constituted by the independent comb and two semi-infinite leads. This conservation rule enables to find all the states of the final system and in particular the bound ones [28].

Another approach to systems build out of one-dimensional pieces is known as quantum graphs [32,33]. This approach calculates directly eigenvalues and eigenfunctions and their continuity conditions. Interface response theory uses the well-known Green's function defined for the Maxwell wave equation. This theory satisfies automatically the boundary condition in agreement with the quantum graph theory. Interface response theory enables to obtain all the hidden states of any system, thanks to the state phase and the state number conservation.

In Sec. II, we present the interface response theory of continuous media. In Sec. III are derived the states of the unperturbed comb structure (Fig. 1) without the leads. Section IV gives the results obtained for the unperturbed and perturbed comb with two leads: BIC, SIBIC states, transmission, transmission phase, state phase shift, and long-lived

transmission resonances. In Sec. V, we present a detailed theoretical study of a quasi-one-dimensional system. The aim of this section is to present BICs and SIBICs in a simple system using interface response theory. Section VI is devoted to study the highly directional outputs through two different lines of a comb structure (Fig. 9, see below). In each output line two different long-lived resonances enable to transmit two different signals. This system enables to demultiplex four different signals, two through one output line and the two other through another output line. The conclusions and prospective are presented in Sec. VII.

## II. INTERFACE RESPONSE THEORY OF CONTINUOUS MEDIA

### A. Overview

In this paper, we study the propagation of electromagnetic waves in composite systems composed of one-dimensional continuous segments (or branches) grafted on two connected guides (see Fig. 1). This study is performed with the help of the interface response theory [34] of continuous media, which permits us to calculate the Green's function of any composite material. In what follows, we present the basic concepts and the fundamental equations of this theory.

Let us consider any composite material contained in its space of definition  $D$  and formed out of  $N$  different homogeneous pieces situated in their domains  $D_i$ . Each piece is bounded by an interface  $M_i$ , adjacent in general to  $j$  ( $1 \leq j \leq J$ ) other pieces through subinterface domains  $M_{ij}$ . The ensemble of all these interface spaces  $M_i$  will be called the interface space  $M$  of the composite material.

The elements of the Green's function  $g(DD)$  of any composite material can be obtained from [34]

$$g(DD) = G(DD) - G(DM)G^{-1}(MM)G(MD) + G(DM)G^{-1}(MM)g(MM)G^{-1}(MM)G(MD), \quad (1)$$

where  $G(DD)$  is the Green's function of a reference continuous medium and  $g(MM)$  the interface elements of the Green's function of the composite system. The inverse  $g^{-1}(MM)$  of  $g(MM)$  is obtained for any points in the space of the interfaces  $M = \{\cup M_i\}$  as a superposition of the different  $g_i^{-1}(M_i, M_i)$  [34,35] inverse of the  $g_i(M_i, M_i)$  for each constituent  $i$  of the composite system. The latter quantities are given by the equation

$$g_i^{-1}(M_i, M_i) = \Delta(M_i, M_i)G_i^{-1}(M_i, M_i), \quad (2)$$

where

$$\Delta(M_i, M_i) = I(M_i, M_i) + A_i(M_i, M_i), \quad (3)$$

$I$  is the unit matrix and

$$A_i(X, X') = V_i(X'')G_i(X'', X')|_{X''=X}, \quad (4)$$

where  $\{X, X''\} \in M_i$  and  $X' \in D_i$ .

In Eq. (4), the cleavage operator  $V_i$  acts only in the surface domain  $M_i$  of  $D_i$  and cuts the finite or semi-infinite size block out of the infinite homogeneous medium [34].  $A_i$  is called the surface response operator of block  $i$ .

The new interface states can be calculated from [34]

$$\det[g^{-1}(MM)] = 0 \quad (5)$$

showing that if one is interested in calculating the interface states of a composite, one only needs to know the inverse of the Green's function of each individual block in the space of their respective surfaces and/or interfaces.

Moreover, if  $U(D)$  [36] represents an eigenvector of the reference system, Eq. (1) enables one to calculate the eigenvectors  $u(D)$  of the composite material as

$$u(D) = U(D) - U(M)G^{-1}(MM)G(MD) + U(M)G^{-1}(MM)g(MM)G^{-1}(MM)G(MD). \quad (6)$$

In Eq. (6),  $U(D)$ ,  $U(M)$ , and  $u(D)$  are row vectors. Equation (6) enables one also to calculate all the waves reflected and transmitted by the interfaces as well as the reflection and the transmission coefficients of the composite system. In this case,  $U(D)$  must be replaced by a bulk wave launched in one homogeneous piece of the composite material.

### B. Inverse surface Green's functions of the elementary constituents

We report here the expression of the Green's function of a homogeneous isotropic infinite dielectric medium. For the sake of simplicity, we restrict ourselves to nonmagnetic homogeneous guide. We give also the inverse of the surface Green's function for the semi-infinite guide with a free surface and for the finite guide of length  $L$ .

#### 1. Green's function of an infinite guide

The Maxwell electromagnetic wave differential equation for the electric field  $\mathbf{E}$  enabling us to obtain electromagnetic waves in an infinite one-dimensional guide without charges or electric currents is

$$\left( \frac{\partial^2}{\partial x^2} - \frac{1}{c^2} \frac{\partial^2}{\partial t^2} \right) E(x, t) = 0, \quad (7)$$

where  $x$  is the space position along the guide,  $t$  is the time, and  $c$  is the electromagnetic wave speed within the guide.

The response function  $G(x, x')$  of this infinite guide is defined by

$$\left( \frac{\partial^2}{\partial x^2} - \frac{1}{c^2} \frac{\partial^2}{\partial t^2} \right) G(x, x') = \delta(x - x')\delta(t - t'), \quad (8)$$

where  $\delta$  stands for the Dirac delta distribution, also known as the unit impulse.

The corresponding response function is

$$G(x, x') = \frac{e^{i\alpha|x-x'|}}{2i\alpha}, \quad (9)$$

where

$$\alpha = \frac{2\pi}{\lambda}. \quad (10)$$

$\lambda$  is the photonic wavelength related to the electromagnetic wave frequency  $\omega$  by  $\lambda = 2\pi c/\omega$  and  $i^2 = -1$ .

#### 2. Semi-infinite guide

One considers a semi-infinite guide with a "free surface" located at the position  $x = 0$  in the direction  $Ox$  of the

Cartesian coordinates. In this case [37]

$$g_s^{-1}(MM) = g_s^{-1}(00) = i\alpha. \quad (11)$$

#### 3. Finite guide

One considers a finite guide of length  $L$  bounded by two free surfaces located on  $x = 0$  and  $x = L$  in the direction  $Ox$  of the Cartesian coordinates system. In this case [37]

$$g_L^{-1}(MM) = \frac{\alpha}{S} \begin{pmatrix} -C & 1 \\ 1 & -C \end{pmatrix} = \begin{pmatrix} g_L^{-1}(00) & g_L^{-1}(0L) \\ g_L^{-1}(L0) & g_L^{-1}(LL) \end{pmatrix}, \quad (12)$$

where  $C = C(L) = \cos(\alpha L)$  and  $S = S(L) = \sin(\alpha L)$ .

One can see that in the interface domain  $M$  corresponding to interfaces  $x = 0$  and  $x = L$ , the surface Green's function is a  $2 \times 2$  square matrix. In order to study elementary electromagnetic excitations, we calculate the surface Green's function for different composite systems composed of finite segments grafted on a one-dimensional wave guide.

### III. TWO ARM THREE PORT COMB STATES

The comb structure without the leads described in Fig. 1 is composed of guides connected together. Use is made of mono-mode guides. The photon wavelengths are large compared to the size of the comb interface sites. Amplification and attenuation can be easily introduced, if needed for comparisons with systems made out of coaxial cables, optical fibers, or micro and nano devices.

#### A. Green's function components

Before giving the states of the comb without the leads, we will recall briefly the expression of the Green's function of the different guides from which the comb structure is composed, namely:

(i) The matrix inverse of  $g_L^{-1}(MM)$  [see Eq. (12)] is given by

$$g_L(MM) = \frac{1}{\alpha S} \begin{pmatrix} C & 1 \\ 1 & C \end{pmatrix}, \quad (13)$$

and is the interface response matrix. The elements of this matrix gives the interface response functions

$$g_L(00) = g_L(11) = C/(\alpha S), \quad (14a)$$

$$g_L(01) = g_L(10) = 1/(\alpha S). \quad (14b)$$

(ii) Interface response function for a backbone composed of two guides: The inverse of the Green's (response) function  $g_{2L}^{-1}(MM)$  in the space of interface  $M = \{-1, 0, 1\}$  [Fig. 2(b)] of two guides (of length  $2L$  each) connected at site zero is given by the linear superposition of the  $(2 \times 2)$  matrices given in Eq. (12) for each of the independent guides constituting the backbone [28],

$$g_{2L}^{-1}(MM) = \frac{\alpha}{S(2L)} \begin{pmatrix} -C(2L) & 1 & 0 \\ 1 & -2C(2L) & 1 \\ 0 & 1 & -C(2L) \end{pmatrix}, \quad (15)$$

where  $C(2L) = \cos(2\alpha L)$ ,  $S(2L) = \sin(2\alpha L)$ ,  $\alpha = 2\pi/\lambda$ , and  $\lambda$  is the photonic wavelength.

(iii) Interface response function for the comblike structure without leads: The inverse of the Green's (response) function

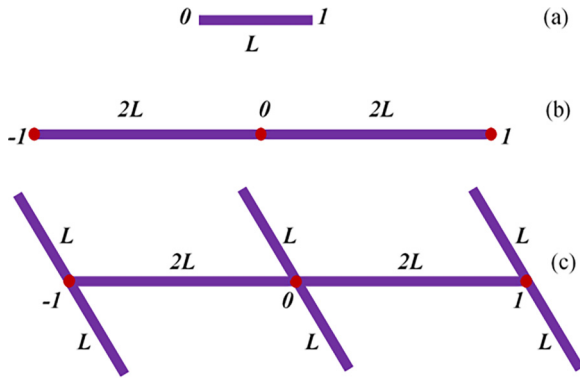


FIG. 2. (a) Finite guide of length  $L$ . The point 0 (or 1) is the point of connection of this guide with the other world. This is why we call it *interface point*. The *interface space* for this finite guide is the two points 0 and 1. This interface space is written shortly as  $M_L = \{0, 1\}$ . (b) A backbone composed of two guides. The length of each guide is  $2L$ . The *interface space* for this backbone is  $M = \{-1, 0, 1\}$ . (c) The same as in (b) but with two stubs of length  $L$  each, connected at the interface points  $M = \{-1, 0, 1\}$ . This is the comb structure (without the semi-infinite leads) studied in this paper.

$g^{-1}(MM)$  in the space of interface  $M = \{-1, 0, 1\}$  of the comb structure (without leads and in the case of  $\delta = 0$ ) is given by the linear superposition of the  $(2 \times 2)$  matrices given in Eq. (12) for each of the independent guides constituting the comb [Fig. 2(c)] [28],

$$g_c^{-1}(MM) = g_{2L}^{-1}(MM) + 2 \begin{pmatrix} g_L^{-1}(-1, -1) & 0 & 0 \\ 0 & g_L^{-1}(00) & 0 \\ 0 & 0 & g_L^{-1}(11) \end{pmatrix}. \quad (16)$$

Using Eqs. (13) and (15), one obtains

$$g_c^{-1}(MM) = \alpha \begin{pmatrix} Y_1 & Y_3 & 0 \\ Y_3 & Y_2 & Y_3 \\ 0 & Y_3 & Y_1 \end{pmatrix}, \quad (17)$$

where  $Y_1 = -\frac{C(2L)}{S(2L)} + 2\frac{S(L)}{C(L)}$ ,  $Y_2 = -2\frac{C(2L)}{S(2L)} + 2\frac{S(L)}{C(L)}$ , and  $Y_3 = \frac{1}{S(2L)}$ . A simple algebra leads to

$$|g_c^{-1}(MM)| = \frac{\alpha^3}{2SC^3} (6S^2 - 1)(12S^2 - 5). \quad (18)$$

(iv) Interface response function for the comblike structure with the leads: The inverse of the Green's (response) function  $g_f^{-1}(MM)$  in the space of interface  $M = \{-1, 0, 1\}$  of the comb structure studied in this paper is given by

$$g_f^{-1}(MM) = g_c^{-1}(MM) + 2 \begin{pmatrix} 0 & 0 & 0 \\ 0 & g_s^{-1}(0, 0) & 0 \\ 0 & 0 & 0 \end{pmatrix}, \quad (19)$$

where the symbol  $f$  refers to any final structure composed of independent guides.

Using Eqs. (11) and (19), one obtains

$$g_f^{-1}(MM) = \alpha \begin{pmatrix} Y_1 & Y_3 & 0 \\ Y_3 & Y_2 + 2i & Y_3 \\ 0 & Y_3 & Y_1 \end{pmatrix}. \quad (20)$$

For the case of nonzero  $\delta$ , one simply repeats the above procedure and use the proper length for each guide.

The inverse of the matrix given in Eq. (20) is the interface response matrix. The elements of this matrix gives the interface response functions. A simple algebra leads to the interface response function

$$g(00) = \frac{\alpha^{-1}C(L)[3C(2L) - 2]}{2[3S(3L) - 4S(L)] + i[3C(3L) - C(L)]} = \frac{(2\alpha)^{-1}C(6S^2 - 1)}{S(12S^2 - 5) + iC(6S^2 - 1)}, \quad (21)$$

used in the calculations of the transmission and reflection functions.

(v) The inverse of the Green's (response) function  $g^{-1}(MM)$  in the space of interface  $M = \{-1, 0, 1\}$  (Fig. 1) of the comb structure (with  $\delta \neq 0$  and without the leads) is given by the linear superposition of the  $(2 \times 2)$  matrices given above in Eq. (12) for each of the independent guides constituting the comb [28],

$$g^{-1}(MM) = \alpha \begin{pmatrix} a_{-1} & b_{-1} & 0 \\ b_{-1} & a_0 & b_1 \\ 0 & b_1 & a_1 \end{pmatrix}, \quad (22)$$

where

$$a_{-1} = \frac{S[2(L - 3\delta)]}{C(L - 2\delta)C(L - 4\delta)} - \frac{C[2(L - \delta)]}{S[2(L - \delta)]}, \quad (23)$$

$$a_0 = \frac{S(2L)}{C(L + \delta)C(L - \delta)} - \frac{2C(2L)S(2L)}{S[2(L - \delta)]S[2(L + \delta)]}, \quad (24)$$

$$a_1 = \frac{S[2(L + 3\delta)]}{C(L + 2\delta)C(L + 4\delta)} - \frac{C[2(L + \delta)]}{S[2(L + \delta)]}, \quad (25)$$

$$b_{-1} = \frac{1}{S[2(L - \delta)]}, \quad (26)$$

and

$$b_1 = \frac{1}{S[2(L + \delta)]}. \quad (27)$$

The boundary conditions are: the continuity of the wave functions and the vanishing at each space point of the sum of the outgoing first derivatives of the field [28]. The eigenfunction derivatives produce source forces. For each eigenstate, the sum of these forces has to vanish at each space point, concerned by this state [28]. For each state, the sum of all surface forces created by this state, has also to vanish. These conditions are implicitly taken into account in the framework of interface response theory [31].

## B. States of the unperturbed comb ( $\delta = 0$ )

The reference system of the unperturbed comb structure presented in Fig. 2(c) is composed of eight independent guides. For each finite guide of length  $L$ , the discrete states are given by the poles of the Green's function, namely  $\alpha S(L) = 0$  [see Eq. (13)], therefore the initial states of the

system composed of 8 independent guides are given by  $(\alpha S(L))^6(\alpha S(2L))^2 = 0$ .

We have also for each finite guide [using Eq. (12)], the determinant of the surface Green function is given by  $|g_L^{-1}(MM)| = -\alpha^2$ . Therefore, for the reference system [see Fig. 2(c)],  $g_R^{-1}(MM) = (-\alpha^2)^8 = \alpha^{16}$ . In addition, the determinant of the matrix given by Eq. (17) is given by Eq. (18).

So the final states of the system without leads are given by the state number conservation and the state phase shift [28] to be

$$(\alpha S)^6(\alpha SC)^2 \frac{|g_c^{-1}(MM)|}{(\alpha^2)^2(\alpha S/C)^6} = 0, \quad (28)$$

that is,

$$\alpha SC^5[6S^2 - 1][12S^2 - 5] = 0. \quad (29)$$

For  $\alpha = 0$ , we have the invariant by translation state [1,1,1]. The path states of such a system without the leads are given by  $SC^5 = 0$ .

The  $S = 0$  state eigen wavelengths are  $\lambda = 2L/n$ , where  $n = 0, 1, 2, 3, \dots$ . Their state eigenvectors are localized within the whole structure. The  $C^5 = 0$  state eigen wavelengths are  $\lambda = 4L/(1 + 2n)$ . Their state eigenvector localizations are for three of these states within the two stubs attached to each of the three ports of this comb. Each of them has a specific eigenfunction zero at its corresponding port. The fourth  $C = 0$  state eigenvector is localized between two nearest-neighbor ports, including one stub on each of these two ports. It has robust zeros on these two ports. The fifth  $C = 0$  state eigenvector is localized between the 1 and -1 ports including one stub on each of these two ports. It has robust zeros on the three ports of this comb. The  $S^2 = 1/6$  states have robust zeros on the three comb ports. The  $S^2 = 5/12$  states have no robust zero on the comb ports.

#### IV. BIC, SIBIC STATES, AND TRANSMISSION

##### A. BIC states

According to the above results and to the BIC and SIBIC state theorems given in our previous paper [30], the structure of Fig. 1 has the following BIC states:

The  $C^5 = 0$  are five times degenerate BIC states, when leads are added to the comb ports. Three of them are localized each within two of the twin stubs of length  $L$ . They have a robust zero on the port to which they are attached. The fourth  $C = 0$  BIC state is localized between two nearest-neighbor ports including one stub attached to each of these two ports. It has robust zeros on these two ports. The fifth  $C = 0$  BIC state is localized between the 1 and -1 ports including one stub on each of these two ports. It has robust zeros on the three ports of this comb. We have to keep in mind that any other linear sum of these five  $C = 0$  states is also a valid state. This analysis also shows that on each of the three sites  $(-1, 0, 1)$ , we have a double robust zero due to two different  $C = 0$  BIC states. The  $S^2 = 1/6$  BIC states have also robust zeros on all three comb ports. In order to make these BIC states pop out when plotting the transmission curve we have to break the symmetry of the comb structure shown in Fig. 1. As shown on Fig. 1, one tuning parameter  $\delta$  enable to change all the comb distances.

##### B. SIBIC states

Another important effect is that each port stub may create one SIBIC state, when a lead is connected to this port. For example when one lead is attached at site 1 to the symmetry broken comb of Fig. 1, it is possible to obtain up to two SIBIC states, as two different finite branches start from this port. Each SIBIC state induces a transmission zero and contributes to one long-lived resonance.

The leads attached to site 0 transform the matrix given by Eq. (22) into

$$g^{-1}(MM) = \alpha \begin{pmatrix} a_{-1} & b_{-1} & 0 \\ b_{-1} & a_0 + 2i & b_1 \\ 0 & b_1 & a_1 \end{pmatrix}, \quad (30)$$

The determinant of the above matrix (for  $\delta = 0$ ) is given by

$$|g^{-1}(MM)| = \frac{\alpha^3}{2S^2C^3}(6S^2 - 1)[S(12S^2 - 5) + iC(6S^2 - 1)]. \quad (31)$$

Taking into account the state number conservation and the BIC and SIBIC theorems (given in our previous paper [30]), the BIC states of the final system can be confirmed to be given by

$$C^5(6S^2 - 1) = 0. \quad (32)$$

In each of the two reference semi-infinite leads there is only one state for each value of  $\lambda$  [28]. Only a comb state with nonzero eigenvector values at the connection point between leads and comb interacts with the state continua. The connection of such a comb state with the lead states give rise to a resonance peak within the variations of the density of states, and the transmission curves.

##### C. Transmission

Equation (6) allows us to calculate the transmission coefficient of the composite system depicted in Fig. 1. Consider now an incident wave  $U(x) = e^{-iax}$ , launched in the left semi-infinite lead. From Eqs. (6) and (30), one can obtain the transmission function in the right semi-infinite lead for the unperturbed comb, namely,  $t = -2i\alpha g(0, 0)$ , or equivalently,

$$t = \frac{C(6S^2 - 1)}{C(6S^2 - 1) - iS(12S^2 - 5)}. \quad (33)$$

In the same way, the reflection function in the left semi-infinite lead is given by  $r = 2i\alpha g(0, 0) - 1$ . From the expressions of  $t$ , one can deduce the transmission coefficient as  $T = |t|^2$ . When  $S(L) = \pm\sqrt{1/6}$  or  $C(L) = 0$  the transmission  $T$  equals zero. The variation of  $T$  (for the unperturbed comb) vs  $2L/\lambda$  is reported in Fig. 3 (dashed plot). The eigen wavelengths of the transmission zeros given by  $S(L) = \pm\sqrt{1/6}$  and  $C(L) = 0$  correspond to the eigenmodes of the comb without the leads.

The transmission (in dashed-plot) vs  $2L/\lambda$  in dimensionless units is drawn in Fig. 3 for the unperturbed comb ( $\delta = 0$ ). It repeats periodically to infinity. Note the transmission 1 due the bulk states  $S(L) = 0$  and  $S(L) = \pm\sqrt{5/12}$ . The solid line plot presents mostly seven new very sharp long-lived resonances, due to the reference seven BIC states.

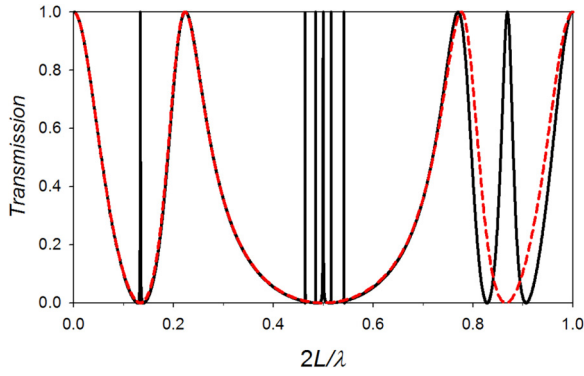


FIG. 3. Transmission (in dashed-plot) vs  $2L/\lambda$  in dimensionless units for the unperturbed comb ( $\delta = 0$ ), with five BIC states localized in the comb for  $C^5(L) = 0$  and  $6S^2 = 1$ . The solid line plot (for perturbed comb with  $\delta = 0.025$ ) shows mostly seven new very sharp long-lived resonances, due to the reference seven BIC states.

In Fig. 4 we show the variation of the transmission coefficient (with color scale) vs  $2L/\lambda$  (in dimensionless units) and the tuning parameter  $\delta$ . The sharp dip close to  $2L/\lambda = 0.865$  indicates the position of the BIC state corresponding to  $S(L) = -\sqrt{1/6}$ . This figure shows for one of the seven long-lived resonances how the width of these resonances can be tuned. The color code given on the right of this figure enables to understand how this resonance decreases in function of  $2L/\lambda$ .

It is well known that the eigenmodes of the system are given by the poles of the Green's function, or for the transmission active ones, by the poles of the transmission

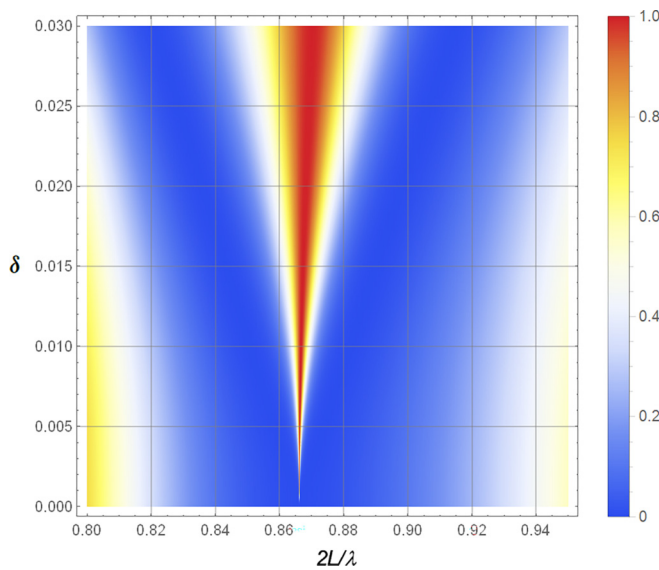


FIG. 4. Variation of the transmission coefficient (with color scale) vs  $2L/\lambda$  (in dimensionless units) and the tuning parameter  $\delta$ . The sharp dip close to  $2L/\lambda = 0.865$  indicates the position of the BIC state corresponding to  $S(L) = -\sqrt{1/6}$ . This figure shows for one of the seven long-lived resonances how the width of these resonances can be tuned. The color code given on the right enables to understand how this resonance decreases in function of  $2L/\lambda$ .

function  $t$  [Eq. (33)], namely,

$$C(6S^2 - 1) - iS(12S^2 - 5) = 0. \quad (34)$$

This latter equation is a complex quantity, its real part gives the position of the BIC states in the transmission and density of states, whereas its imaginary part is related to the width of the resonances and also here to the transmission active states.

#### D. Transmission phase and state phase shift for the unperturbed comb

The transmission phase is obtained from Eq. (33) to be

$$\phi = \tan^{-1} \left[ \frac{S(12S^2 - 5)}{C(6S^2 - 1)} \right]. \quad (35)$$

Another interesting quantity is the first derivative of  $\phi$  with respect to  $2L/\lambda$ , which is related to the delay time taken by the photons to traverse the structure. This quantity, called phase time, is defined by [38]

$$\tau_\phi = \frac{d\phi}{d(2L/\lambda)}. \quad (36)$$

Moreover, another interesting entity that can be extracted from the Green's function is the bulk state phase shift  $\eta$ . This bulk state phase shift between the final system (the comb with the leads) and the reference system (the eight independent guides and the two semi-infinite leads) is given by [31]

$$\eta = -\arg\{\det\{g^{-1}(MM)\}\}. \quad (37)$$

From Eq. (31) one can deduce that

$$\eta = -\tan^{-1} \left[ \frac{C(6S^2 - 1)}{S(12S^2 - 5)} \right]. \quad (38)$$

In order to provide an analytical comparison of the density of states with the phases involved in the system, we consider the variation of the density of states (VADOS)  $\Delta n(2L/\lambda)$  between the final system depicted in Fig. 1 and the reference system composed of the eight guides and the two semi-infinite leads. This quantity is given by [31]

$$\Delta n(2L/\lambda) = -\frac{1}{\pi} \frac{d\eta}{d(2L/\lambda)}. \quad (39)$$

Note that the  $\pi$  drops in  $\phi$  and  $\eta$  are due to the zero values of the denominators appearing in their respective analytical expressions. As these denominators are not the same, the  $\eta$  and  $\phi$ ,  $\pi$  drop positions are not the same.

In Fig. 5(a) we plot the bulk state phase shift vs  $2L/\lambda$  for the unperturbed structure ( $\delta = 0.0$ ). The two  $\pi$  drops (close to  $2L/\lambda = n$ , where  $n$  is an integer) are due to the loss of two bulk states out of the four reference  $12S^2 - 5$  ones. The remaining two of these four states induce two resonant peaks, as shown by the transmission curve in dashed-plot, superposed here. The other  $\pi$  drops are induced by the  $S(L) = 0$  states and the corresponding resonances. Figure 5(b) shows the VADOS vs  $2L/\lambda$ . Note the negative delta peaks due to the loss of  $S(L) = 0$  and  $12S^2 - 5 = 0$  states. We introduced the dissipation in the system by adding a small imaginary part to  $2/\lambda$ , i.e.,  $2/\lambda$  becomes  $2/\lambda \pm j(0.0001)$ . Introducing this

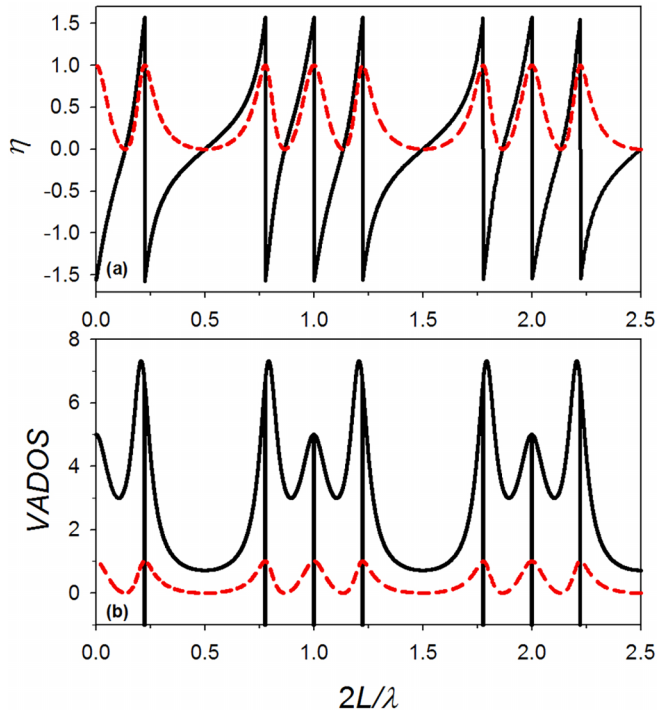


FIG. 5. (a) Bulk state phase shift vs  $2L/\lambda$  for the unperturbed structure ( $\delta = 0.0$ ). The two  $\pi$  drops (close to  $2L/\lambda = n$ , where  $n$  is an integer) are due to the loss of two bulk states out of the four reference  $12S^2 - 5$  ones. The remaining two of these four states induce two resonant peaks, as shown by the transmission curve in dashed-plot, superposed here. The other  $\pi$  drops are induced by the  $S(L) = 0$  states and the corresponding resonances. (b) VADOS vs  $2L/\lambda$ . Note the negative delta peaks due to the loss of  $S(L) = 0$  and  $12S^2 - 5 = 0$  states. We introduced the dissipation in the system by adding a small imaginary part to  $2/\lambda$ , i.e.,  $2/\lambda$  becomes  $2/\lambda \pm j(0.0001)$ . Introducing this imaginary part makes the negative delta peaks show up in the VADOS plot.

imaginary part make the negative delta peaks show up in the VADOS plot.

In Fig. 6(a) bulk state phase shift vs  $2L/\lambda$  is plotted for the perturbed structure ( $\delta = 0.025$ ). The  $\pi$  drop (at  $2L/\lambda \simeq 0.87$ ) is due to the loss of one bulk state induced by one of the  $12S^2 = 5$  reference states. The remaining one of these two times degenerate reference states induces one resonant peak. This  $\pi$  drop is associated with a maximum in the transmission curve in dashed-plot, superposed here for agreement check. Figure 6(b) shows the VADOS vs  $2L/\lambda$ . The negative delta pic is due to the loss of one of the  $12S^2 = 5$  states. The dashed curve recalls the transmission curve.

Figure 7(a) shows the transmission phase vs  $2L/\lambda$  for the unperturbed structure. The  $\pi$  drops at  $2L/\lambda = 0.5, 1.5, \dots$  are induced by the  $C = 0$  SIBIC states while the other  $\pi$  drops are induced by the  $6S^2 = 1$  BIC states. The transmission phase exhibits, a phase jump at the transmission zeros. Figure 7(b) shows the phase time vs  $2L/\lambda$ . The phase time and the VADOS are exactly the same, when one neglects the derivatives of the  $\pi$  drops. This happens only when one has two leads. We introduced the dissipation in the system by adding a small imaginary part to  $2/\lambda$ , i.e.,  $2/\lambda$  becomes

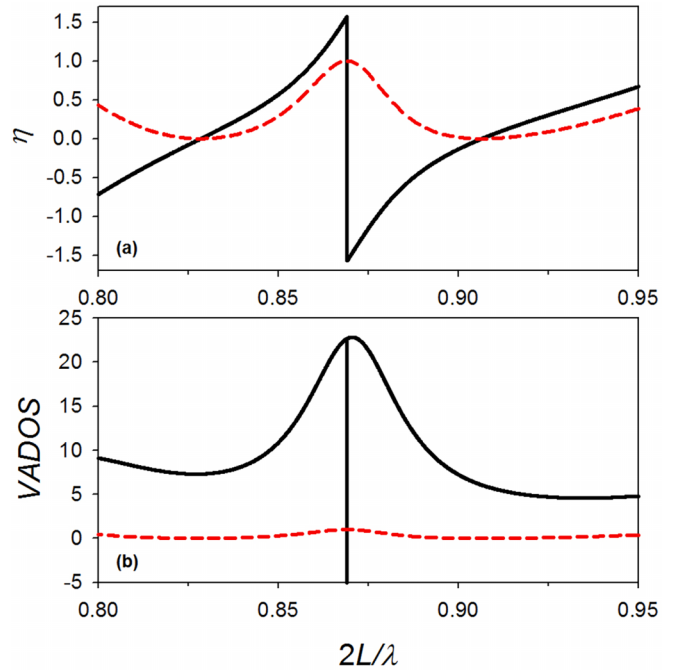


FIG. 6. (a) Bulk state phase shift vs  $2L/\lambda$  for the perturbed structure ( $\delta = 0.025$ ). The  $\pi$  drop (at  $2L/\lambda \simeq 0.87$ ) is due to the loss of one bulk state induced by one of the  $12S^2 = 5$  reference states. The remaining one of these two times degenerate reference states induces one resonant peak. This  $\pi$  drop is associated with a maximum in the transmission curve in dashed-plot, superposed here for agreement check. (b) VADOS vs  $2L/\lambda$ . The negative delta pic is due to the loss of one of the  $12S^2 = 5$  states. The dashed curve recalls the transmission curve.

$2/\lambda \pm j(0.0001)$ . Introducing this imaginary part make the negative delta peaks show up in the phase time plot. The dashed curve recalls the transmission one, for agreement checks.

Figure 8(a) shows the transmission phase vs  $2L/\lambda$  for the perturbed structure ( $\delta = 0.025$ ). The  $\pi$  drops are induced by the new SIBIC states, due to the robust zeros. This provides one single positive peak and two negative delta ones, in the phase time, see Fig. 8(b). Figure 8(b) shows the Phase time vs  $2L/\lambda$ . The phase time and the VADOS are exactly the same, when one neglects the derivatives of the  $\pi$  drops. This happens only when one has two leads.

## V. SIMPLE CASE: TWO FINITE GUIDES

In recent years, BICs in a simple cavity attracted much interest [39–41]. In this section, we present a simple system consisting of two finite guides grafted onto two semi-infinite guides at a single point (point 0, see Fig. 9). This system features BICs and SIBICs, which will be discussed in detail in this section. The superposition at the interface point 0 of the two reference elements (two finite guides of lengths  $L - \delta$  and  $L + \delta$ ) of the final finite system of Fig. 9 provides the inverse of the  $g(0, 0)$  response function element of the final system to



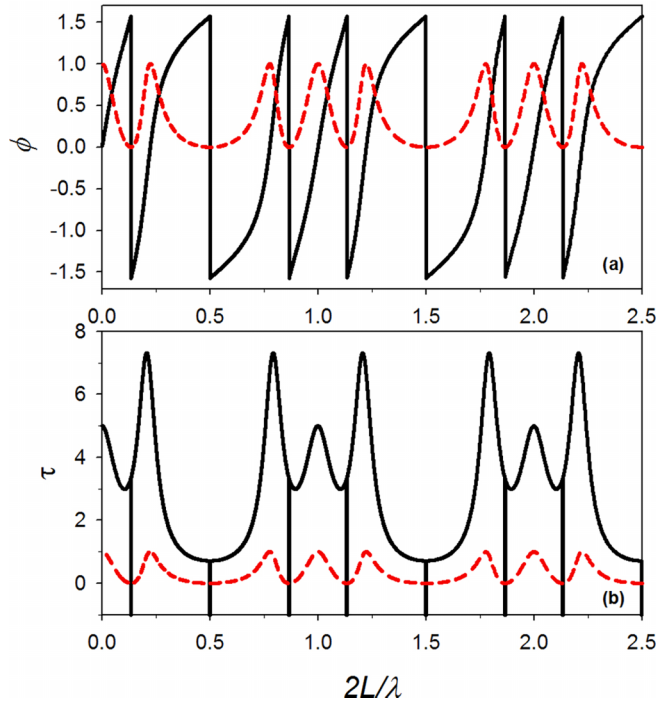


FIG. 7. (a) Transmission phase vs  $2L/\lambda$  for the unperturbed structure. The  $\pi$  drops at  $2L/\lambda = 0.5, 1.5, \dots$  are induced by the  $C = 0$  SIBIC states while the other  $\pi$  drops are induced by the  $6S^2 = 1$  BIC states. The transmission phase exhibits, a phase jump at the transmission zeros. (b) Phase time vs  $2L/\lambda$ . The Phase time and the VADOS are exactly the same, when one neglects the derivatives of the  $\pi$  drops. This happens only when one has two leads. We introduced the dissipation in the system by adding a small imaginary part to  $2/\lambda$ , i.e.,  $2/\lambda$  becomes  $2/\lambda \pm j(0.0001)$ . Introducing this imaginary part makes the negative delta peaks show up in the phase time plot. The dashed curve recalls the transmission one, for agreement checks.

be [see Eq. 14(a)]

$$\begin{aligned} g^{-1}(0, 0) &= \alpha \left[ \frac{S(L - \delta)}{C(L - \delta)} + \frac{S(L + \delta)}{C(L + \delta)} \right] \\ &= \frac{2\alpha S(L)C(L)}{C(L - \delta)C(L + \delta)}. \end{aligned} \quad (40)$$

The corresponding reference expression is

$$g_R^{-1}(0, 0) = \frac{\alpha^2 S(L - \delta)S(L + \delta)}{C(L - \delta)C(L + \delta)}. \quad (41)$$

The reference system states are given by

$$\alpha^2 S(L - \delta)S(L + \delta) = 0. \quad (42)$$

The state phase shift is obtained from the state number conservation rule to be

$$\eta_0 = \arg \left( \frac{|g(00)|}{|g_R(00)|} \right). \quad (43)$$

The above equations enable to confirm that the finite final system states are given by

$$\alpha S(L)C(L) = 0. \quad (44)$$

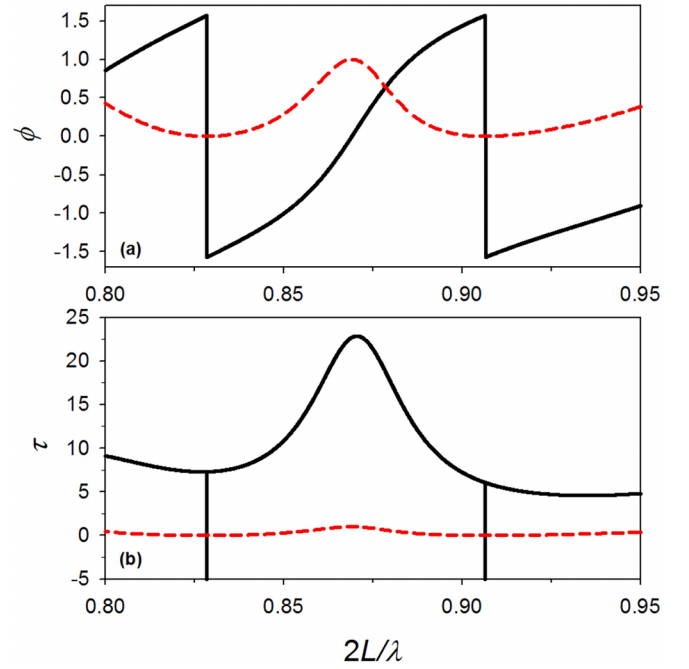


FIG. 8. (a) Transmission phase vs  $2L/\lambda$  for the perturbed structure ( $\delta = 0.025$ ). The  $\pi$  drops are induced by the new SIBIC states, due to the robust zeros. This provides one single positive peak and two negative delta ones, in the phase time, see (b). (b) Phase time vs  $2L/\lambda$ . The Phase time and the VADOS are exactly the same, when one neglects the derivatives of the  $\pi$  drops. This happens only when one has two leads.

Equations (40) and (44) enable to find, on the interface site 0, the eigenvectors of the states. The  $g^{-1}(0, 0)$  is a  $(1 \times 1)$  matrix, so its eigenvectors  $u$  are defined by

$$g^{-1}(0, 0)u = 0. \quad (45)$$

So in this case, when  $\delta \neq 0$ , the eigenvectors are 1 for all eigenvalues  $\alpha S(L)C(L) = 0$ . Remark also that this matrix diverges when  $C(L - \delta)C(L + \delta) = 0$ , which corresponds to forced states of the reference system two elements. It is interesting to notice, at this stage, that for these forced states, the value of  $u$  is 0.

Let us add now the two semi-infinite leads. The inverse of the  $g(0, 0)$  response function element of the final system is

$$g^{-1}(0, 0) = \alpha \left[ \frac{2S(L)C(L)}{C(L - \delta)C(L + \delta)} + 2i \right]. \quad (46)$$

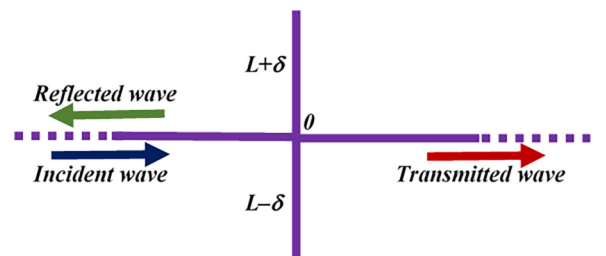


FIG. 9. The cross system with two finite guides.

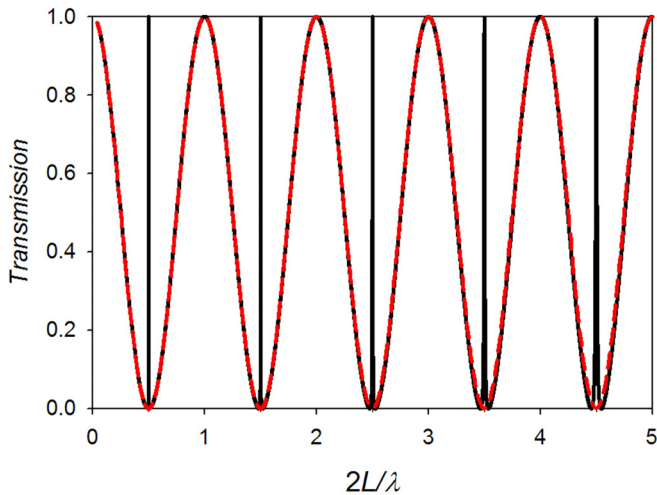


FIG. 10. The two curves give the transmission coefficient  $T$  function of  $2L/\lambda$ . The dashed plot is for  $\delta = 0$  and  $L = 1$ . The solid line is for  $\delta = 0.01$ . Each very sharp long-lived resonance, in the second case, is bound by transmission zeros due to two SIBIC states  $2L/\lambda = (1 + 2n)(L/2(L - \delta))$  and  $2L/\lambda = (1 + 2n)(L/2(L + \delta))$ , where  $n$  is a positive integer.

The reference forced states of the guides are

$$C(L - \delta)C(L + \delta) = 0, \quad (47)$$

when  $\delta \neq 0$ , become SIBIC eigenstates in the final system. Their eigenfunctions can connect with one of the two semi-infinite leads. At their interface robust zeros, they can fulfill their derivative boundary condition only with one semi-infinite lead. And because of their interface robust zeros, these SIBIC states induce transmission zeros.

Let us stress here that these SIBIC states are created out of discrete reference forced states. The forced states do not exist as eigenstates in the reference system. They induce the  $C(L) = 0$  states of the open loop  $2L$ , which become BIC states, in the final system, when  $\delta = 0$ .

Figure 10 shows such two SIBIC states localized each within one semi-infinite lead and one finite guide. These SIBIC states can not connect with the other lead and the other finite guide because of their eigenfunction zeros at the corresponding interface.

The bulk state phase shift is

$$\eta\left(\frac{2L}{\lambda}\right) = -\tan^{-1}\left(\frac{C(L - \delta)C(L + \delta)}{S(L)C(L)}\right). \quad (48)$$

The above equation enabled already to conclude that the discrete  $S(L)C(L) = 0$  states of a finite guide of length  $2L$  are lost in the final system. In the final system, with  $\delta = 0$ , the  $C(L) = 0$  are BIC states, localized within the two stubs.

In the reference system, each semi-infinite lead has one set of  $S(L) = 0$  states. In the final system, for the sake of state number conservation one set of  $S(L) = 0$  states, localized within the whole final system, appears. But there is no  $C(L) = 0$  states left in the final system, when  $\delta \neq 0$ .

Consider the variation of the density of states  $\Delta n(2L/\lambda)$  between the final system depicted in Fig. 9 and the reference system composed of the two finite guides and the two

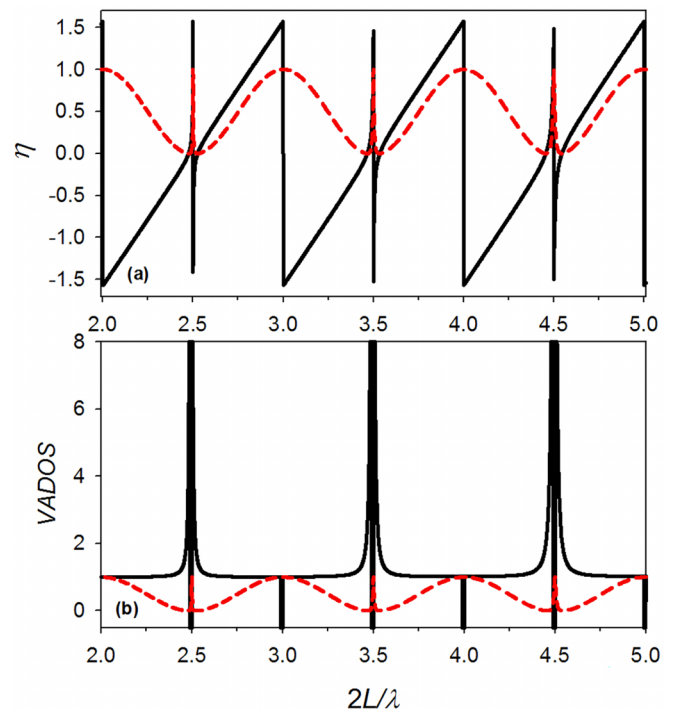


FIG. 11. A simple example of bulk state phase shift and VADOS induced by two SIBIC states. The upper solid line curve gives the state phase shift  $\eta$  function of  $2L/\lambda$ . The bottom curve presents the VADOS. The transmission (dashed) curve is superposed on both. The parameters are  $L = 1$  and  $\delta = 0.01$ . Note the  $\pi$  drops and the state losses for  $2L/\lambda = n/2$ , as well as the sharp corresponding peaks within the VADOS.

semi-infinite leads. This quantity is given by [31]

$$\Delta n\left(\frac{2L}{\lambda}\right) = \frac{1}{\pi} \frac{d\eta}{d(2L/\lambda)}. \quad (49)$$

The transmission function  $t$  is obtained from

$$t = 2i\alpha g(0, 0), \quad (50)$$

the transmission coefficient from

$$T = |t|^2 = \frac{4C^2(L - \delta)C^2(L + \delta)}{4C^2(L - \delta)C^2(L + \delta) + S^2(2L)}, \quad (51)$$

and the transmission phase from

$$\phi = \tan^{-1}\left(\frac{S(L)C(L)}{C(L - \delta)C(L + \delta)}\right). \quad (52)$$

Another interesting quantity is the first derivative of  $\phi$  with respect to  $2L/\lambda$ , which is related to the delay time taken by the photons to traverse the finite system. This quantity, called phase time, is defined by

$$\tau_\phi = \frac{d\phi}{d(2L/\lambda)}. \quad (53)$$

In Fig. 10, the two curves give the transmission coefficient  $T$  function of  $2L/\lambda$ . The plot in dashed plot is for  $L = 1$  and  $\delta = 0$ . The one in solid line is for  $\delta = 0.01$ . The transmission ones are obtained when  $S(2L) = 0$  and the transmission zeros when  $C(L - \delta) = 0$  and  $C(L + \delta) = 0$ . Each very-sharp long-lived resonance, in the second case, is bound by transmission

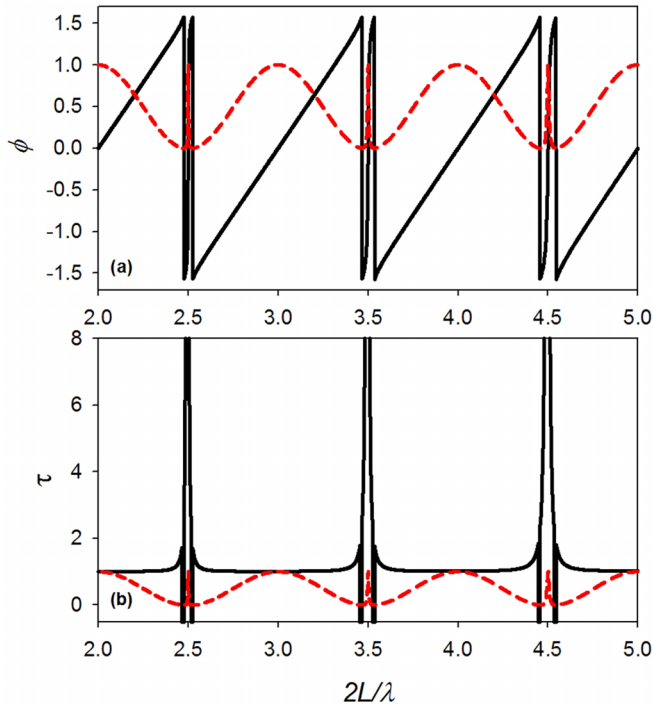


FIG. 12. A simple example of the transmission phase and the phase time induced by two SIBIC states. The upper solid line curve gives the transmission phase  $\phi$  function of  $2L/\lambda$ . The bottom solid line curve presents the phase time  $\tau_\phi$ . The transmission  $T$  in dashed plot is superposed on both for agreement checks. The parameters are  $\delta = 0.01$  and  $L = 1$ . Note the  $\pi$  drops due to the nonparticipating to transmission SIBIC states and the peaks they induce in the phase time.

zeros due to two SIBIC states  $2L/\lambda = (1 + 2n)(L/2(L - \delta))$  and  $2L/\lambda = (1 + 2n)(L/2(L + \delta))$ , where  $n$  is a positive integer.

Figure 11 presents the state phase shift and the VADOS, as simple examples of effects induced by two SIBIC states. The upper solid line curve gives the state phase shift  $\eta$  function of  $2L/\lambda$ . The bottom solid line curve presents the VADOS. The transmission curve is superposed on both. The parameters are  $L = 1$  and  $\delta = 0.01$ . Note the  $\pi$  drops and the state losses for  $2L/\lambda = n/2$ , as well as the sharp corresponding peaks within the VADOS.

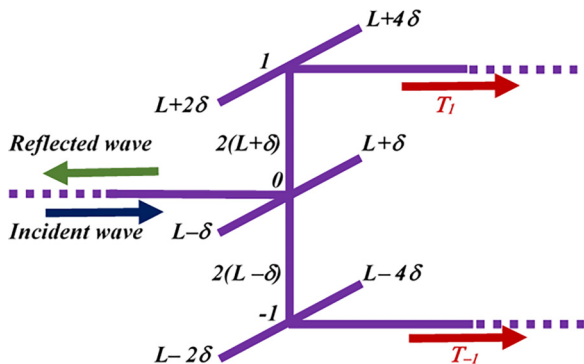


FIG. 13. Comb demultiplexer structure with one input lead and two output ones.

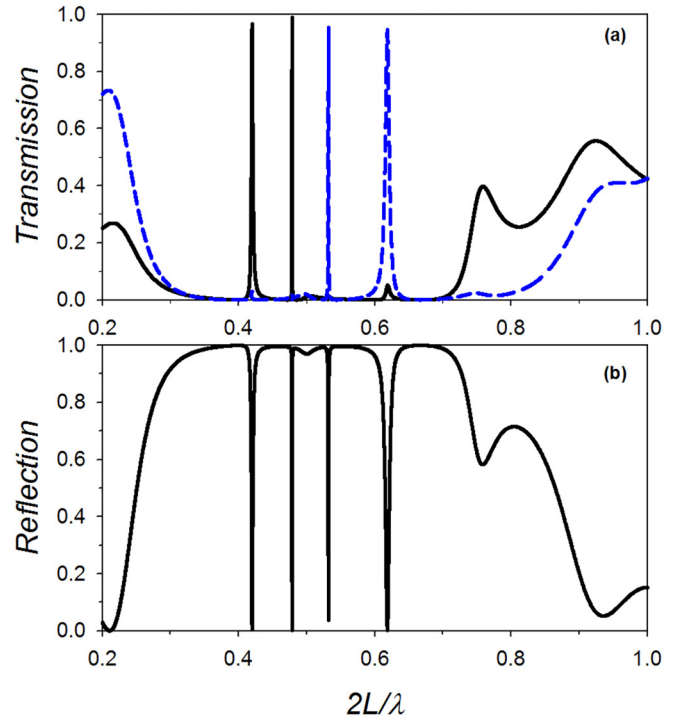


FIG. 14. The transmissions and reflection through the comb demultiplexer. All unperturbed branches have a length  $L = 1$ . The perturbation  $\delta$  values are here equal to  $\delta = 0.2$  for the two branches connecting site 0 to sites 1 and  $-1$ ,  $\delta_0 = 0.25$  for the two stubs attached to site 0,  $\delta_1 = 0.02$  for the two stubs attached to site 1 and  $\delta_{-1} = 0.015$  for the two stubs attached to site  $-1$ . Panel (a) shows in dashed plot the transmission output through site 1 and in solid line the output through site  $-1$ . Note that this system enables to directionally transmit two different signals through each of the two output lines. Panel (b) shows the corresponding reflection long-lived resonances.

Figure 12 presents the transmission phase and the phase time. This is a simple example of the transmission phase and the phase time induced by two SIBIC states. The upper solid line curve gives the transmission phase  $\phi$  function of  $2L/\lambda$ . The down solid line curve presents the phase time  $\tau_\phi$ . The transmission  $T$  is superposed on both figures. The parameters are  $L = 1$  and  $\delta = 0.01$ . Note the  $\pi$  drops due to the nonparticipating to transmission SIBIC states and the peaks they induce in the phase time.

## VI. DIRECTIONAL OUTPUT OF LONG-LIVED RESONANCES

The above comb structure is now used with one input line at site 0 and two output lines at sites 1 and  $-1$ , as shown by Fig. 13.

Figure 14 shows the transmissions and reflection through this comb demultiplexer. All unperturbed branches have a length  $L = 1$ . The perturbation  $\delta$  values are here equal to  $\delta = 0.2$  for the two branches connecting site 0 to sites 1 and  $-1$ ,  $\delta_0 = 0.25$  for the two stubs attached to site 0 and  $\delta_{-1} = 0.015$  for the two stubs attached to site  $-1$ . Figure 14(a) shows in dashed line

plot the transmission  $T_1$  through site 1 and in solid line the transmission  $T_{-1}$  through site  $-1$ . Note that this system enables to directionally transmit two different signals through each of the two output lines. Figure 14(b) shows the corresponding reflection long-lived resonances.

## VII. CONCLUSIONS AND PROSPECTIVE

The above simple comb structure has seven BIC states. It may be tuned to show seven very sharp long-lived resonances. The number of the BIC states and long-lived resonances may be increased by adding more arms to this comb structure.

It may be used for the construction of a type of demultiplexer able to transmit directly two independent signals through each of two output leads. It is possible also by adding more arms to this structure to get more than two independent signals per output line and more different such output lines.

This paper is also a simple example of how to find all the states, including the BIC ones, for any final system. This is

achieved with the state phase and the state number conservation between a final system and its reference one. This method is completely general and is expected to be used in future investigations of BIC states and long-lived resonances.

Indeed the majority of present investigations are done with topological simulation approaches focusing on small deformations and one BIC state. Although introducing the state phase within the numerical routines is not trivial, this is expected to complete and improve their results.

Indeed the knowledge of all system BIC states, rather than only one, enables to choose the better one for a given application. This may help also to use several degenerate BIC states for novel devices.

## ACKNOWLEDGMENT

H.A.-W. and E.A.A.-G. gratefully acknowledge the hospitality of the Institut d'Electronique, de Microelectronique et de Nanotechnologie (IEMN), UMR CNRS 8520 and UMR 9189 CRISAL, F-59000, Université de Lille, France.

- 
- [1] J. von Neuman and E. Wigner, Über das Verhalten von Eigenwerten bei adiabatischen Prozessen, *Phys. Z.* **30**, 467 (1929).
- [2] U. Fano, Effects of configuration interaction on intensities and phase shifts, *Phys. Rev.* **124**, 1866 (1961).
- [3] M. Fleischhauer, A. Imamoglu, and J. P. Marangos, Electromagnetically induced transparency: Optics in coherent media, *Rev. Mod. Phys.* **77**, 633 (2005).
- [4] J. Jiang, Q. Zhang, Q. Ma, S. Yan, F. Wu, and X. He, Dynamically tunable electromagnetically induced reflection in terahertz complementary graphene metamaterials, *Opt. Mater. Express* **5**, 1962 (2015).
- [5] Q. Song, L. Ge, J. Wiersig, and H. Cao, Formation of long-lived resonances in hexagonal cavities by strong coupling of superscar modes, *Phys. Rev. A* **88**, 023834 (2013).
- [6] C. W. Hsu, B. Zhen, A. D. Stone, J. D. Joannopoulos, and M. Soljačić, Bound states in the continuum, *Nat. Rev. Mater.* **1**, 16048 (2016).
- [7] A. A. Bogdanov, K. L. Koshelev, P. V. Kapitanova, M. V. Rybin, S. A. Gladyshev, Z. F. Sadrieva, K. B. Samusev, Y. S. Kivshar, and M. F. Limonov, Bound states in the continuum and Fano resonances in the strong mode coupling regime, *Adv. Photon.* **1**, 016001 (2019).
- [8] F. He, J. Liu, G. Pan, F. Shu, X. Jing, and Z. Hong, Analogue of electromagnetically induced transparency in an all-dielectric double-layer metasurface based on bound states in the continuum, *Nanomaterials* **11**, 2343 (2021).
- [9] L. Huang, Y. K. Chiang, S. Huang, C. Shen, F. Deng, Y. Cheng, B. Jia, Y. Li, D. A. Powell, and A. E. Miroshnichenko, Sound trapping in an open resonator, *Nat. Commun.* **12**, 4819 (2021).
- [10] M. Amrani, I. Quotane, C. Ghouila-Houri, E. H. El Boudouti, L. Krutyanskiy, B. Piwakowski, P. Pernod, A. Talbi, and B. Djafari-Rouhani, Experimental Evidence of the Existence of Bound States in the Continuum and Fano Resonances in Solid-Liquid Layered Media, *Phys. Rev. Appl.* **15**, 054046 (2021).
- [11] I. Quotane, E. H. El Boudouti, and B. Djafari-Rouhani, Trapped-mode-induced Fano resonance and acoustical transparency in a one-dimensional solid-fluid phononic crystal, *Phys. Rev. B* **97**, 024304 (2018).
- [12] A. Mouadili, E. H. El Boudouti, A. Akjouj, H. Al-Wahsh, B. Djafari-Rouhani, and L. Dobrzynski, Effect of damping on magnetic induced resonances in cross waveguide structures, *J. Supercond. Novel Magn.* **34**, 597 (2021).
- [13] T. Mrabti, Z. Labdouti, A. Mouadili, E. El Boudouti, and B. Djafari-Rouhani, Aharonov-Bohm-effect induced transparency and reflection in mesoscopic rings side coupled to a quantum wire, *Physica E* **116**, 113770 (2020).
- [14] E. N. Bulgakov, K. N. Pichugin, A. F. Sadreev, and I. Rotter, Bound states in the continuum in open Aharonov-Bohm rings, *JETP Lett.* **84**, 430 (2006).
- [15] S. Sun, Y. Ding, H. Li, P. Hu, C.-W. Cheng, Y. Sang, F. Cao, Y. Hu, A. Alù, D. Liu, Z. Wang, S. Gwo, D. Han, and J. Shi, Tunable plasmonic bound states in the continuum in the visible range, *Phys. Rev. B* **103**, 045416 (2021).
- [16] Z. Qi, G. Hu, B. Liu, Y. Li, C. Deng, P. Zheng, F. Wang, L. Zhao, and Y. Cui, Plasmonic nanocavity for obtaining bound state in the continuum in silicon waveguides, *Opt. Express* **29**, 9312 (2021).
- [17] S. Xie, S. Xie, J. Zhan, C. Xie, G. Tian, Z. Li, and Q. Liu, Bound states in the continuum in a t-shape nanohole array perforated in a photonic crystal slab, *Plasmonics* **15**, 1261 (2020).
- [18] S. T. Ha, Y. H. Fu, N. K. Emani, Z. Pan, R. M. Bakker, R. Paniagua-Domínguez, and A. I. Kuznetsov, Directional lasing in resonant semiconductor nanoantenna arrays, *Nat. Nanotechnol.* **13**, 1042 (2018).
- [19] L. L. Doskolovich, E. A. Bezus, and D. A. Bykov, Integrated flat-top reflection filters operating near bound states in the continuum, *Photon. Res.* **7**, 1314 (2019).
- [20] X. Cui, H. Tian, Y. Du, G. Shi, and Z. Zhou, Normal incidence filters using symmetry-protected modes in dielectric subwavelength gratings, *Sci. Rep.* **6**, 36066 (2016).
- [21] F. Wu, J. Wu, Z. Guo, H. Jiang, Y. Sun, Y. Li, J. Ren, and H. Chen, Giant Enhancement of the Goos-Hänchen Shift Assisted

- by Quasibound States in the Continuum, *Phys. Rev. Appl.* **12**, 014028 (2019).
- [22] D. Conteduca, I. Barth, G. Pitruzzello, C. P. Reardon, E. R. Martins, and T. F. Krauss, Dielectric nanohole array metasurface for high-resolution near-field sensing and imaging, *Nat. Commun.* **12**, 3293 (2021).
- [23] X. Zhao, C. Chen, K. Kaj, I. Hammock, Y. Huang, R. D. Averitt, and X. Zhang, Terahertz investigation of bound states in the continuum of metallic metasurfaces, *Optica* **7**, 1548 (2020).
- [24] J. F. Algorri, F. Dell’Olio, P. Roldán-Varona, L. Rodríguez-Cobo, J. M. López-Higuera, J. M. Sánchez-Pena, and D. C. Zografopoulos, Strongly resonant silicon slot metasurfaces with symmetry-protected bound states in the continuum, *Opt. Express* **29**, 10374 (2021).
- [25] S. I. Azzam, V. M. Shalaev, A. Boltasseva, and A. V. Kildishev, Formation of Bound States in the Continuum in Hybrid Plasmonic-Photonic Systems, *Phys. Rev. Lett.* **121**, 253901 (2018).
- [26] P. S. Pankin, B. R. Wu, J. H. Yang, K. P. Chen, I. V. Timofeev, and A. F. Sadreev, One dimensional photonic bound states in the continuum, *Commun. Phys.* **3**, 91 (2020).
- [27] L. Dobrzyński, H. Al Wahsh, and A. Akjouj, Photonic open loops, in *Resonance*, edited by L. Dobrzyński (Elsevier, Amsterdam, 2023), pp. 11–52.
- [28] L. Dobrzyński, H. Al-Wahsh, A. Akjouj, and E. H. El Boudouti *et al.*, Photonic paths, in *Photonics*, edited by L. Dobrzyński (Elsevier, Amsterdam, 2021), pp. 1–145.
- [29] L. Dobrzyński, A. Akjouj, G. Lévêque, E. H. El Boudouti, and H. Al-Wahsh, Centered system magnons, in *Magnonics*, edited by L. Dobrzyński (Elsevier, Amsterdam, 2019), pp. 1–51.
- [30] H. Al-Wahsh, L. Dobrzyński, and A. Akjouj, Long-lived resonances: Photonic triangular pyramid, *Photon. Nanostruct.-Fundam. Appl.* **50**, 101022 (2022).
- [31] L. Dobrzynski, A. Akjouj, E. H. El Boudouti, and H. Al-Wahsh *et al.*, Interface response theory, in *Photonics*, edited by L. Dobrzynski (Elsevier, Amsterdam, 2018), pp. 1–18.
- [32] K.-K. Voo and C. S. Chu, Localized states in continuum in low-dimensional systems, *Phys. Rev. B* **74**, 155306 (2006).
- [33] O. Hul, M. Ławniczak, S. Bauch, A. Sawicki, M. Kuś, and L. Sirko, Are Scattering Properties of Graphs Uniquely Connected to Their Shapes? *Phys. Rev. Lett.* **109**, 040402 (2012).
- [34] L. Dobrzynski, Interface response theory of continuous composite materials, *Surf. Sci.* **180**, 489 (1987).
- [35] L. Dobrzynski, Interface response theory of electromagnetism in composite dielectric materials, *Surf. Sci.* **180**, 505 (1987).
- [36] L. Dobrzynski, Interface response theory of continuous composite systems, *Surf. Sci. Rep.* **11**, 139 (1990).
- [37] M. Bah, A. Akjouj, and L. Dobrzynski, Response functions in layered dielectric media, *Surf. Sci. Rep.* **16**, 97 (1992).
- [38] M. Büttiker and R. Landauer, Traversal Time for Tunneling, *Phys. Rev. Lett.* **49**, 1739 (1982).
- [39] M. Amrani, S. Khattou, E. H. El Boudouti, A. Talbi, A. Akjouj, L. Dobrzynski, and B. Djafari-Rouhani, Friedrich-Wintgen bound states in the continuum and induced resonances in a loop laterally coupled to a waveguide, *Phys. Rev. B* **106**, 125414 (2022).
- [40] E. H. El Boudouti, A. Akjouj, B. Djafari-Rouhani, A. Talbi, and L. Dobrzyński, Electromagnetic induced transparency, induced absorption, and Fano resonances in photonic circuits, in *Photonics*, edited by L. Dobrzyński *et al.* (Elsevier, Amsterdam, 2021), pp. 155–191.
- [41] M. Amrani, S. Khattou, H. Al-Wahsh, Y. Rezzouk, El Houssaine El Boudouti, C. Ghouila Hourri, A. Talbi, A. Akjouj *et al.*, Bound states in the continuum and Fano resonances in photonic and plasmonic loop structures, *Opt. Quantum Electron.* **54**, 599 (2022).